



Original Article

Electrochemical Polymerization of Eugenol and Corrosion Protection Studies of Stainless Steel 304L Alloy

Ayat Monther Alqudsi*, Khulood Abed Saleh

Department of Chemistry, College of Science, Baghdad University, Jaderyah, Baghdad, Iraq

ARTICLE INFO

Article history

Receive: 2022-10-03

Received in revised: 2022-11-07

Accepted: 2022-12-12

Manuscript ID: JMCS-2211-1871

Checked for Plagiarism: Yes

Language Editor:

Dr. Fatimah Ramezani

Editor who approved publication:

Dr. Behrooz Maleki

DOI:10.26655/JMCHMSCI.2023.8.10

KEYWORDS

Electropolymerization

Eugenol

PolyEugenol

Stainless Steel 304L

Nanomaterials

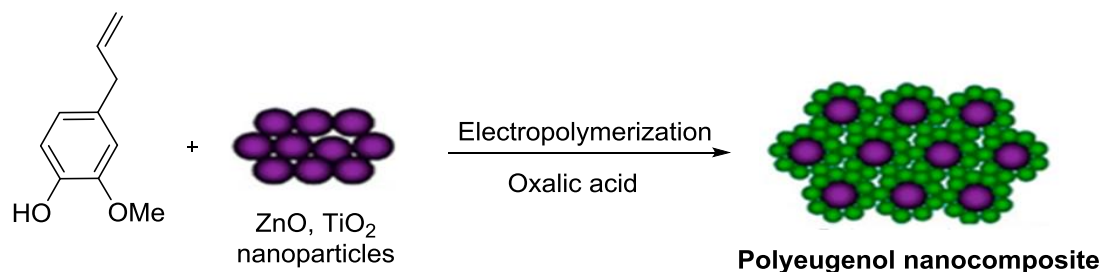
ZnO

TiO₂

ABSTRACT

This research includes the preparation of a poly-eugenol layer on the surface of a stainless steel electrode by electropolymerization process, where the polymer was diagnosed using infrared spectroscopy and atomic force microscopy. The corrosion measurements of stainless steel 304L electrode were carried out before and after coating with polyeugenol in 3.5% of NaCl solution at four different temperatures in the range 298-328 K. Likewise, this study included the addition of nanomaterials such as ZnO and TiO₂ to increase the efficiency of the polymeric layer formed against corrosion. The biological activity of the polymeric film was tested against bacterial Gram- positive *Staphylococcus aureus* (*Staph.aure*) and Gram-negative *Escherichia coli* (*E.coli*). Furthermore, the coating was treated with nanoparticles (ZnO and TiO₂).

GRAPHICAL ABSTRACT



* Corresponding author: Ayat Monther Alqudsi

✉ E-mail: Email: montherayat@gmail.com

© 2023 by SPC (Sami Publishing Company)

Introduction

Electro-Polymerization is a coating process in which the monomer is polymerized in solution at a collecting substrate. Electrolysis is employed to start the initiation in this process, with the monomer polymerized on-site to a conducting surface. It uses the low molecular weight conductive monomers that are more soluble in the medium and containing carbon chain should have double bond [1]. Monomers such as methyl methacrylate [2], styrene [3], aniline as a poly methyl aniline [4], and pyrrole [5] have all been reported to undergo the electro polymerization.

In clove oil, eugenol (4-allyl-2-methoxyphenol) plays a significant role. Clove (*Syzygium aromaticum*, also known as *Eugenia aromaticum*) may be used for its extraction. It may be further produced through lignin depolymerization [6] and from various plants, including cinnamon bark, Tulsi leaves, turmeric, pepper, ginger, and thyme [7]. Because eugenol is a very important molecule with functional groups that may be polymerized, the production of eugenol-based products is now a common procedure. Three functional groups hydroxy, methoxy, and allyl make up the structure of eugenol, as displayed in Figure 1 [8].

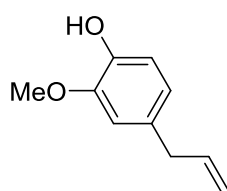


Figure 1: The chemical structure of eugenol

The most popular technique included polymerizing the monomer in a suitable electrolyte to create a thin coating of conductive polymer on stainless steel (the working electrode) [9]. The conductive polymer sheet utilized as an antibacterial and corrosion barrier. The essential characteristics should be presented in the excellent antimicrobial polymers: a-biocidal against a wide range of pathogenic microorganisms, b-it can be regenerated after loss of activity, c-it cannot be soluble in water for various applications and d-it cannot be degraded to the toxic compounds [10, 11].

The self-healing characteristics of composite conducting polymers CP are blended with those of inorganic materials in the CP-based composites. As a result, the composite coatings have better physicochemical and mechanical characteristics, such as increased hydrophobicity, barrier effect, and adhesion [12, 13]. The enhancement of corrosion protection results from the development of these qualities.

Haider A. and Khulood A. indicated that eugenol polymerized on titanium alloys before and after treatment with Micro Arc oxidation was protected from corrosion and the protection efficiency (I%) increased to 81% at 323K. The antimicrobial activities of the samples were

evaluated against various bacteria and oral fungi. Poly Eugenol (PE) coating exhibits antibacterial activity against *S.aureus* and *B.Subtilis*, respectively and antifungal activity against *C.albicans* and *C.glabrata* oral fungi, respectively [11]. A. Ciszewski and G. Milczarek used cyclic voltammetry to modify a platinum electrode with electro-polymerized films of 4-allyl-2-methoxyphenol (eugenol) oxidative polymerization from an alkaline solution, and then the modified electrode was utilized to measure dopamine (DA) levels in an animal [12]. Erwin A. prepared PE with high molecular weight to evaluate its antibacterial and an antioxidant activity, the synthesized PE was weighed using viscometer, in which results indicated a strong antibacterial activity. Then, tests on the antioxidant activity against free radical DPPH (2,2-diphenyl-1-picrylhydrazyl). Therefore, the polymer synthesized (polyeugenol) has a high potential to be applied in various biomedical applications.

In this study, an alkaline electrolyte is used to generate an electropolymerized coating on stainless steel 304L (SS304L) alloys by form a thin layer of poly eugenol (PE) on the surface of SS304L. The FT-IR spectroscopy and AFM measurements were used to analyze the electro-

synthesis of PE coatings, and coating adhesive was evaluated to determine their surface morphologies. In addition, the biological efficacy of PE coating against different bacteria and the oral fungus was investigated.

Materials and Methods

SS304L was used as the working electrode with chemical structure, as described in Table 1.

Samples preparation

SS 304 L specimens of 2×2 cm² area were obtained from commercially stainless steel sheet of 0.5 mm thickness, these samples were polishes with emery papers in different grade including 600, 800, 1200 and 2000 mesh grit, and then washed with tap water, distilled water, ethanol, and finally with acetone, and then they were dried using a hot air drier.

Cyclic voltammetry of PE

A potential of electro-polymerization was determined by cyclic voltammetry. A solution of 10 mM of Eugenol in 0.1 M of NaOH was prepared and three drops added of the concentrated H₂SO₄ to increase the conductivity of electrolyte within potential range between (-2000 to 2000) mV vs. the standard calomel electrode (SCE).

Electro-chemical polymerization of eugenol

The SS 304L working electrodes (anode) was placed in 0.1 M NaOH containing 10 mM eugenol with three drops of H₂SO₄ (99%) and 0.1 g of oxalic acid as supporting electrolyte and it is necessary to use a large rode of graphene as counter electrode (cathode), the voltage of (3 V) was applied at room temperature with duration (90 min.), and then the electrode washed by distilled water and dried by hot air drier [11]. The electrochemical polymerization of the monomer is shown in Figure 2.

Table 1: Chemical composition for SS304L

| material | C | Mn | Si | S | P | Cr | Ni | Fe |
|----------|-------|------|------|-------|-------|-------|------|---------|
| SS 304 L | 0.019 | 1.53 | 0.50 | 0.030 | 0.030 | 18.20 | 8.04 | balance |

Many chemical were used in this work included some regents, as listed in Table 2 with their purity.

Table 2: The used chemical materials

| Raw Material | Molecular Formula | Supplier | Purity |
|---------------------|--|------------------|--------|
| Ethanol | C ₂ H ₅ OH | GCC | 99.9% |
| Eugenol | C ₁₀ H ₁₂ O ₂ | MASTER-DENT | 99.9% |
| Sodium Chloride | NaCl | BDH | 99.5% |
| Sulpharic acid | H ₂ SO ₄ | GCC | 98% |
| Sodium hydroxide | NaOH | BDH | 99% |
| Oxalic acid | H ₂ C ₂ O ₄ | BDH | 99% |
| Nano Zinc Oxide | ZnO | Hongwe nanometer | 99% |
| Nano titanium oxide | TiO ₂ | Hongwe nanometer | 99% |

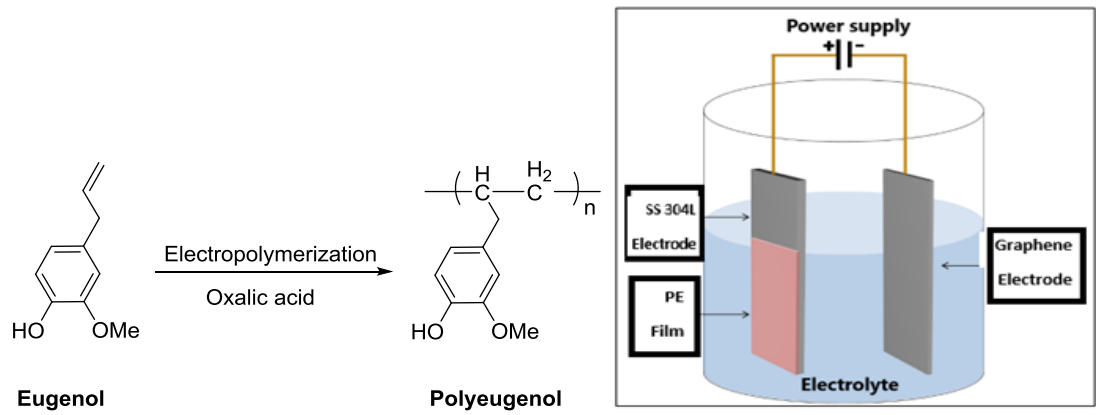
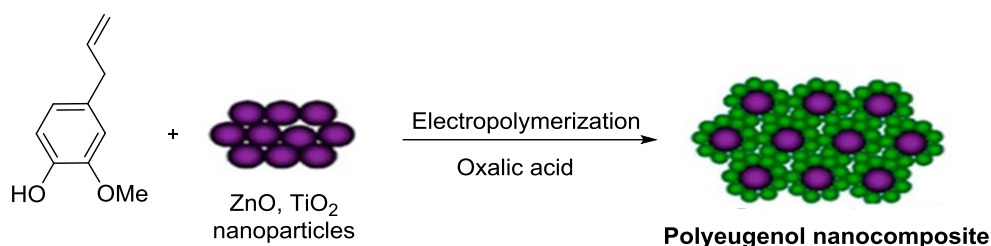


Figure 2: The electropolymerization of eugenol

Effect of nanomaterials

This step includes the nanomaterial addition of (0.01, 0.02, 0.01, 0.03, and 0.04) g to improve the polymer film's efficiency against corrosion and bacteria. The best quantity was 0.02 g of both ZnO and TiO₂ according to the Tafel plots measurements. Therefore, the electropolymerization process was carried out in the

presence of nanomaterials as follows: 10 mM eugenol in 0.1 M of NaOH was prepared with three drops of H₂SO₄ (99%) and 0.1 g of oxalic acid as supporting electrolyte, at room temperature 3 volts was applied with duration 90 min, the electrode was then cleaned with distilled water and dried with hot air [11]. The electrochemical polymerization of the monomer with nanoparticles is depicted in Scheme 1.



Scheme 1: The electrochemical polymerization of the monomer with nanoparticles

Study of electrochemical corrosion

For corrosion studies, a three-electrode cell with a working electrode (SS304 L; before and after coating), a reference electrode (SCE), and a counter, or auxiliary electrode is used (platinum electrode). Anodic and cathodic polarization for corrosion of SS304L was performed in 3.5% NaCl solution under potentiostatic conditions SS304L at temperatures ranging (298-328) K.

Results and Discussion

Cyclic voltammogram of PE

The cyclic voltammogram was taken when the PE film was electro-polymerized on SS 304L and it was utilized to look at the redox characteristics of the polymeric film. The sequential cyclic

voltammogram produced with PE is shown in Figure 3 at around 3.2 volts from the beginning of the scan, an oxidation wave begins that may be related to the beginning of polymerization of monomer. In the subsequent scans, the strength drops of the polymerization wave and it shifts to a higher potential signified the electropolymerization of monomer, when the potential is more than 3.5 v, the rate of polymerization is raised. The reduction peak, which may be associated with the polymer reduction, comes during the reverse potential sweep at 1.5 v. As the polymer coating layer expands, this peak weakens and a subsequent scan shows that the polymer has fully grown. The repeated cycles result in the appearance of a light brown polymer covering.

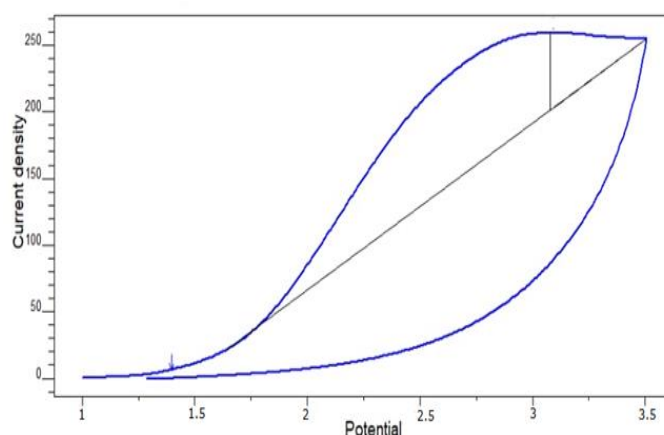


Figure 3: The cyclic voltammogram of PE

Corrosion measurements

Figure 4 demonstrates the typical curves of polarization for the coated and the uncoated SS 304L with polymers in absence and presence of nanomaterial in 3.5% of NaCl solution at a variety of the temperature values (298-328) K. The protective effectiveness was calculated using the following equation (%Pe) [14].

$$\%Pe = [(I_{cor.})_{unc.} - (I_{cor.})_c.] / (I_{cor.})_{unc.} \quad (2)$$

Where, $(I_{cor.})_{unc.}$ is the corrosion current density for blank SS304L (uncoated), $(I_{cor.})_c.$ is the corrosion current density for coated SS304L, obtained by the extrapolation of cathodic and anodic Tafel lines to the corrosion potential. The polarization resistance (R_p) may be determined using the rearranged Stern-Geary Equation [15-19].

$$R_p = \frac{\beta a * \beta b}{(\beta a + \beta b) 2.303} \times \frac{1}{I_c} \quad (3)$$

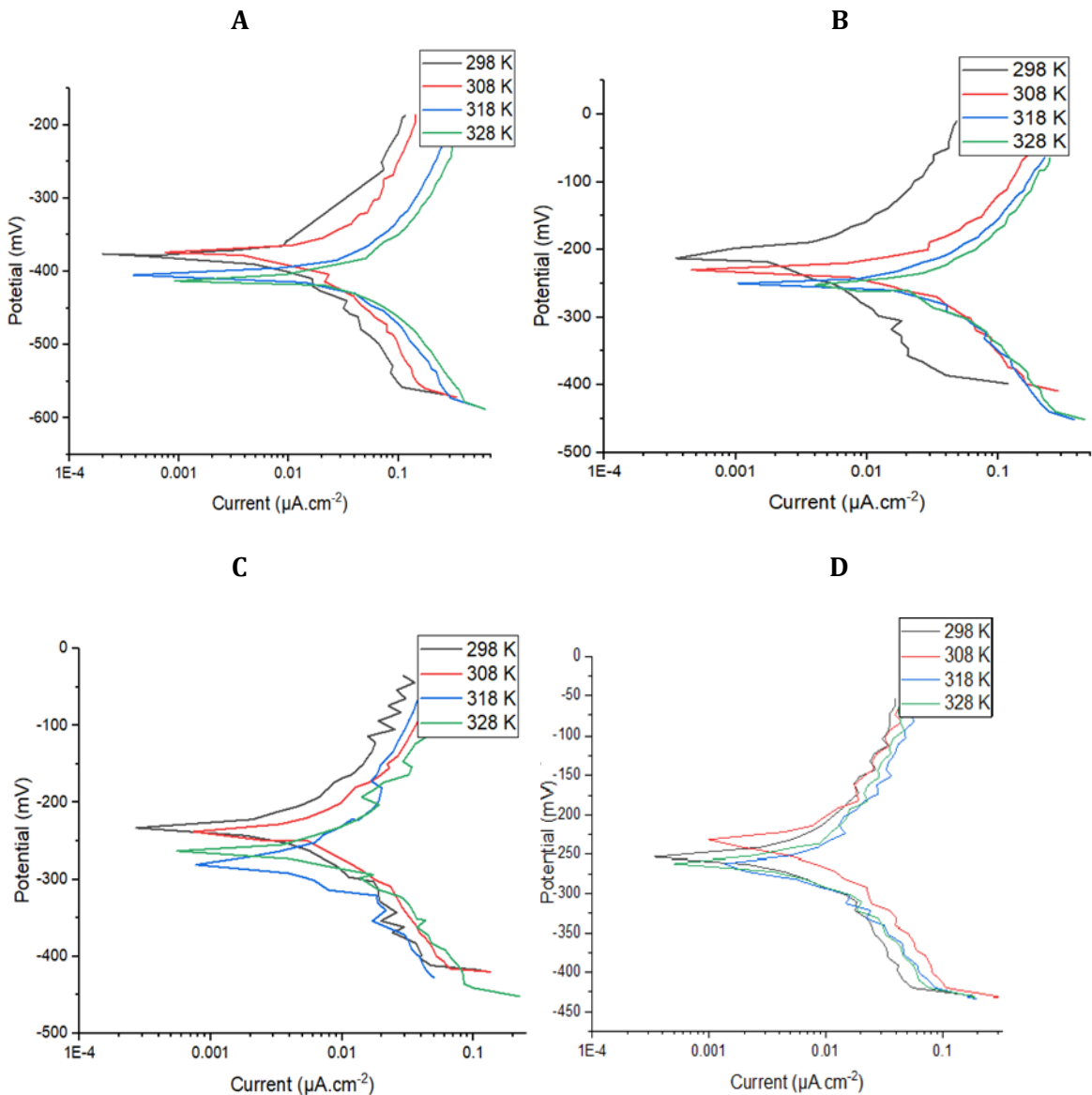


Figure 4: Tafel plots for SS304L (a) uncoated, (b) coated by PE, and (c) coated by PE with ZnO, d) coated by PE with TiO_2

The corrosion potential $E_{cor.}$ and corrosion current density $I_{cor.}$ were extrapolated from the cathodic and anodic Tafel plots of the SS304L that had not been before and after coated with PE in a

solution of 3.5% of NaCl. The anodic βa and cathodic βb Tafel slopes, weight loss WL, penetration loss PL, polarization resistance R_p , and protection efficiency $PE\%$ were also

calculated using Figure 4. The results listed in Table 3 show that both the corrosion potential and current density increased with temperature. When compared to uncoated SS304L, Tafel's plot reveals the coated alloy yield Ecor. moves into a higher location showing that the coating serves as an anodic protection [14].

Measurements of polarization resistance (Rp) have criteria comparable to those of measurements of all polarization curves, and they are a valuable approach for locating corrosion upsets and starting corrective action. Table 3 provides a list of the Rp values.

The anodic and cathodic Tafel slope results obtained are variable at all temperatures. These results are referring to a variation in rate determining the step from the process of charge transfer to the electrochemical desorption and chemical desorption in cathodic reaction and consequently rate determining step variations in the metal dissolution reaction [20].

The values of polarization resistance Rp derived from Equation 3 and shown in Table 3, reduced with temperature for uncoated SS304L and coated SS304L in without and in the presence of

nanomaterials because the bare metal is more conductive than polymer layers [21]. This is because the SS304L surface was nearly completely covered by the nanomaterials. Furthermore, the coating by PE treated with ZnO in NaCl solution at 298 K has the greatest polarization resistance value (13567.83 Ω/cm²). Results in Table 3 indicate that protection efficiency (Pe%) is strongly influenced by temperature, with a fall in Pe% values as temperature increases. This may be explained by the fact that as temperature increases, so did the thickness of the boundary layer [21].

Table 3 reveals that the WL and PL values were greatly dependent on temperature. Temperature had an effect on the WL and PL values, which increased with temperature. All coating systems had the greatest WL and PL values at 328K.

Likewise, the values of WL and PL were lower in coated SS304L than in uncoated SS304L and these values were clearly lower after adding nanomaterial. The porosity of the coating layer and the coating's capacity to inhibit entry of hostile anions such as chloride ion into the surface of S.S. influenced these results [22].

Table 3: Corrosion values for uncoated and coated SS304L with polymer PE

| T(K) | | -E _{cor.} (mV) | I _{cor.} (μA/cm²) | -B _b (mV/ Dec) | β _a (mV/ Dec) | WL (g/m².d) | R _p (Ω/cm²) | PL (mm/y) | Pe% |
|-------------------------------|-----|----------------------------|-------------------------------|---------------------------------|--------------------------------|-----------------------|------------------------|-----------------------|-----|
| Uncoated | 298 | 376 | 8.78 | 124.2 | 130.5 | 2.2 | 3147.13 | 9.79*10 ⁻² | - |
| | 308 | 374 | 21.47 | 160.8 | 155.0 | 5.38 | 1596.17 | 2.40*10 ⁻¹ | - |
| | 318 | 394 | 36.95 | 177.2 | 170.4 | 10.3 | 1020.81 | 4.57*10 ⁻¹ | - |
| | 328 | 405 | 49.57 | 192.1 | 190.4 | 15.4 | 837.62 | 6.87*10 ⁻¹ | - |
| Coated PE | 298 | 211 | 2.72 | 78.6 | 76.1 | 6.82*10 ⁻¹ | 6172.39 | 3.04*10 ⁻² | 69 |
| | 308 | 231 | 7.05 | 75.3 | 77.6 | 1.74 | 2353.78 | 7.75*10 ⁻² | 67 |
| | 318 | 251 | 12.17 | 73.8 | 72.6 | 4.25 | 1305.77 | 1.89*10 ⁻¹ | 65 |
| | 328 | 253 | 19.9 | 72.2 | 71.9 | 5.49 | 786.05 | 2.44*10 ⁻¹ | 60 |
| Coated PE+ZnO EECS | 298 | 232 | 860*10 ⁻³ | 53.2 | 54.3 | 2.16*10 ⁻¹ | 13567.83 | 9.62*10 ⁻³ | 90 |
| | 308 | 260 | 2.86 | 55.0 | 59.6 | 4.66*10 ⁻¹ | 4342.74 | 2.07*10 ⁻² | 86 |
| | 318 | 260 | 6.52 | 78 | 80.4 | 8.73*10 ⁻¹ | 2636.65 | 4.5*10 ⁻² | 82 |
| | 328 | 265 | 9.64 | 95 | 103.1 | 1.41 | 2227.03 | 6.3*10 ⁻² | 80 |
| Coated PE+TiO ₂ | 298 | 234 | 1.66 | 90.6 | 113.2 | 6.67*10 ⁻¹ | 13163.41 | 2.97*10 ⁻² | 81 |
| | 308 | 264 | 4.34 | 89.6 | 98.7 | 8.36*10 ⁻¹ | 4698.84 | 3.72*10 ⁻² | 79 |
| | 318 | 268 | 8.7 | 90.2 | 100.4 | 9.28*10 ⁻¹ | 2371.39 | 4.13*10 ⁻² | 76 |
| | 328 | 264 | 11.95 | 114 | 120.4 | 1.99 | 2127.70 | 8.87*10 ⁻² | 75 |

FT-IR Spectroscopy of the synthesized polymer (PE)

FT-IR spectra (depicted in Figure 5) were recorded for the eugenol monomer and

polyeugenol formed on a SS 304L alloys by electrochemical polymerization. In Figure 4, the absorption bands at 3076 cm⁻¹ are ascribed to asymmetric =CH₂ in eugenol, but this peak cannot found in the polyeugenol IR spectrum. The peak at around 3299 cm⁻¹ can be attributed to intra-molecular H-bonds between the repeating units in polyeugenol chains and this peak cannot found in the eugenol IR spectrum.

Thermodynamic and kinetic activation studies

The corrosion process for uncoated and coated SS304L L in %3.5 of NaCl solution in temperature

range 298-328 K was calculated by using similar Arrhenius Equation [16].

$$I_{cor} = A \exp^{-E_a/RT} \quad (4)$$

This equation was converted into logarithmic form as follows:

$$\log I_{cor} = \log A - \frac{E_a}{2.303 RT} \quad (5)$$

While, the transition state equation is as follows [17, 18]:

$$\log \frac{I_{cor}}{T} = \log \frac{R}{N_h} + \frac{\Delta S}{2.303 R} - \frac{\Delta H}{2.303 RT} \quad (6)$$

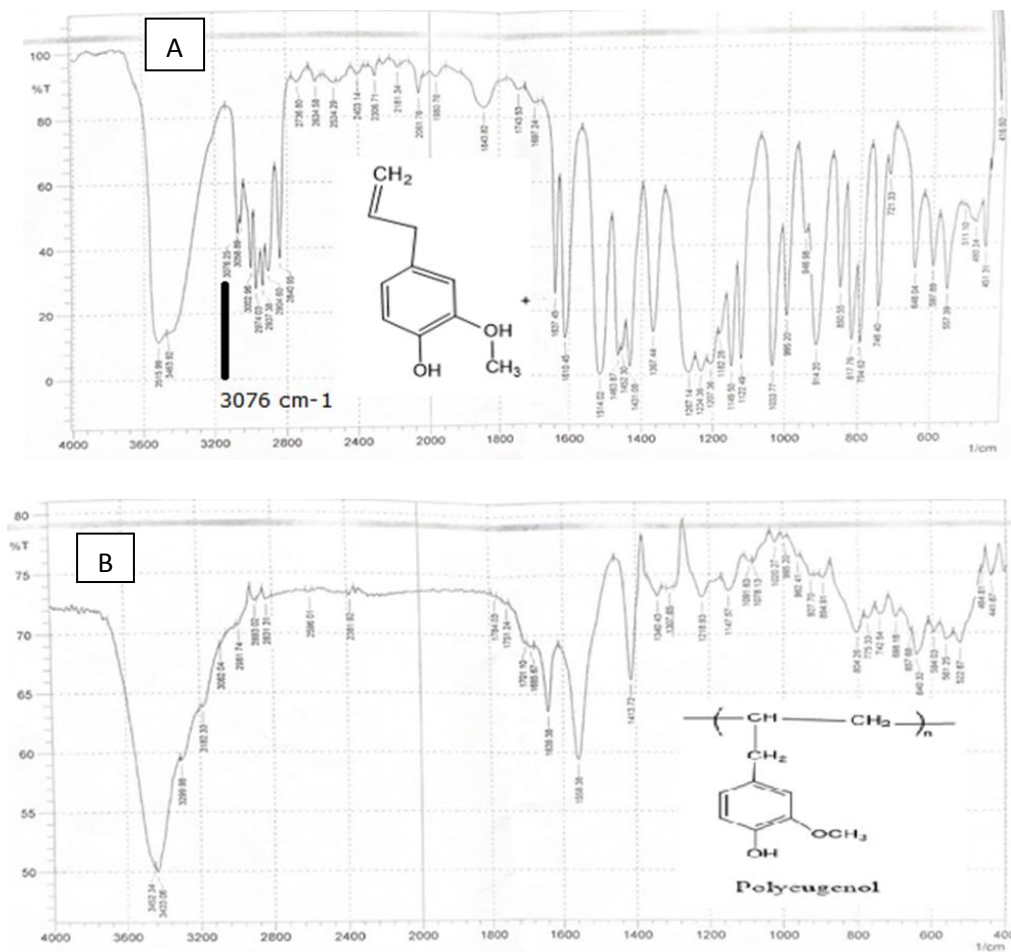


Figure 5: FTIR of (a) Eugenol and (b) PE

Where, R is the universal gas constant equal 8.315 J/K.mol, T is the absolute temperature in K, A is the pre-exponential factor, h is the Planks constant equal 6.62×10⁻³⁴ J.S, N is Avogadros number equal to 6.02×10²³ mol⁻¹, E_a is the activation energy, and (ΔS and ΔH) are the thermodynamic functions (entropy and enthalpy

of activation). The E_a and A values were obtained from slope and intercept, respectively, from the linear regression between Log I_{cor}.vs. 1/T, as demonstrated in Figure 6a, while ΔH and ΔS were obtained from slope and intercept of the linear regression between Log I_{cor}/T vs. 1/T, as illustrated in Figure 6b and listed in Table 4.

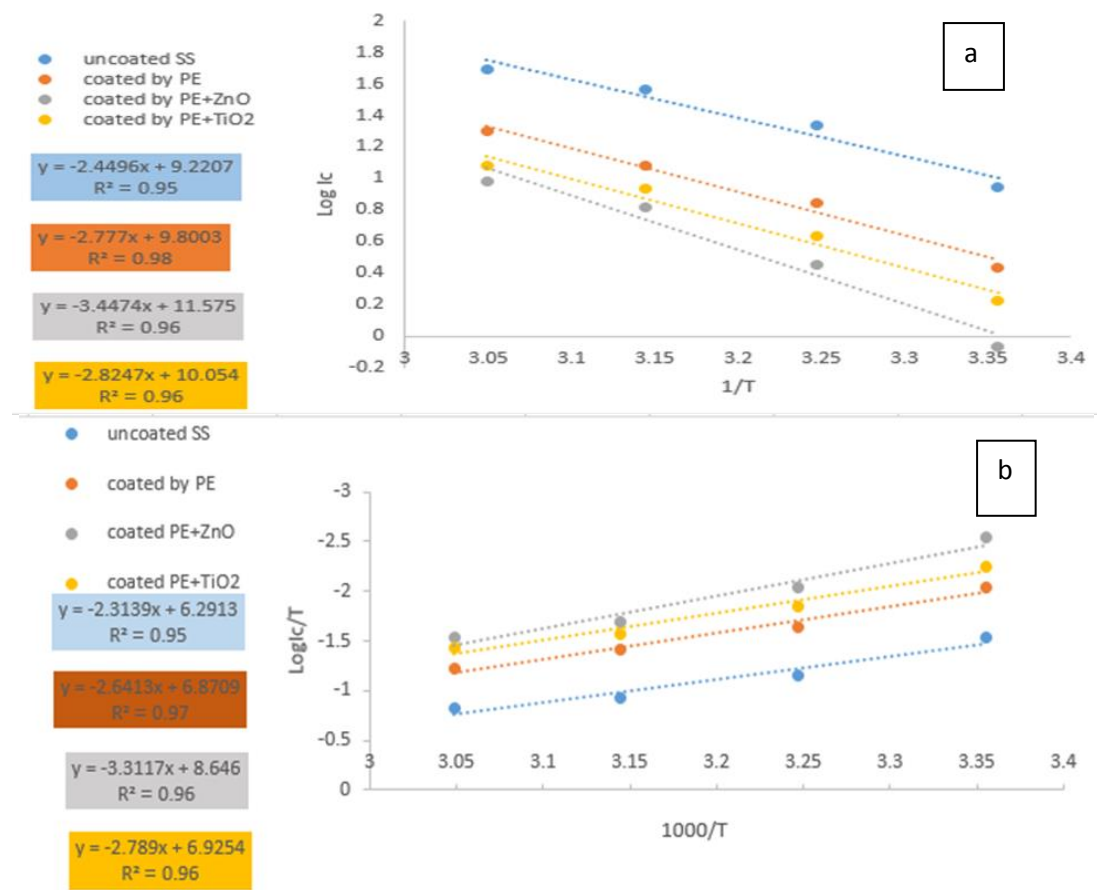


Figure 6: (a) Plot of $\log I_{cor}$ versus $1/T$ for SS304L before and after coating with PE in without and presence of the nanomaterials. (b) Plot of the I_{cor}/T vs. $1/T$ log. SS304L before and after coating with PE in the without and presence of nanomaterials

Table 4: Values of kinetic and thermodynamic for coated and uncoated SS304L with PE in absence and presence of the nanomaterials at different temperatures

| | ΔH^* (kJ/mol) | $-\Delta S^*$ (J/mol.K) | E_a (kJ/mol) | A (Molecule. $\text{Cm}^{-2} \cdot \text{s}^{-1}$) |
|---|-----------------------|-------------------------|----------------|---|
| Uncoated SS 304L | 44.29 | 77.17 | 46.9 | 9.9×10^{32} |
| Coated SS 304L with PE | 50.55 | 66.07 | 53.18 | 0.37×10^{32} |
| Coated SS 304L with PE and ZnO | 63.38 | 32.17 | 66.01 | 2.2×10^{32} |
| Coated SS 304L with PE and TiO ₂ | 53.43 | 64.92 | 54.09 | 6.7×10^{32} |

Table 4 lists all of the estimated values for kinetics and thermodynamic parameters. The findings reveal the activation energies have increased in the presence of the film (PE), which indicates a better protective efficiency of the coating and the values of Arrhenius factor are relatively close to each other as the values refer to the number of corrosion sites on the alloy. After incorporating various nanomaterials into the coating, the activation energies were increased, suggesting a rise in the energy barrier for the corrosion process [23]. The endothermic character of the transition state reaction is shown by the positive activation enthalpies (ΔH^*)

for coated and uncoated SS 304L. The activation complex in the speed determination phase is a combination rather than a dissociation, as shown by the negative values of ΔS^* for coated and uncoated SS304L. This indicates that there is a reduction in disordering when one transitions from reactant to activated complex [24, 25].

Atomic Force Microscope (AFM)

The AFM Technique was used to examine the surface topography of SS 304L coated with PE in the presence and absence of nanomaterials (nano-TiO₂ and nano-ZnO). Figure 7 depicts two and three dimensions AFM pictures of all coating

films applied. Through AFM analysis, the mean grain size, RMS as the root mean square, and Ra as the roughness average are the most often used metrics for determining the surface's roughness. The results indicate that the reduction in grain size caused by the PE treatment with nanoparticles led to a decrease in surface roughness for all coated films, as shown in Table 5. Therefore, the stronger the barrier effect for

preventing corrosion of the coating, the less rough the surface [26].

Antimicrobial Activity of PE

The inhibitory zones of the produced polymers were tested in two species of bacteria *S. aureus* and *E. coli* in the without and in the presence of nanomaterials ZnO and TiO₂ at 800 g/mL. Dimethyl sulfoxide was utilized as the solvent (DMSO), as listed in Table 6.

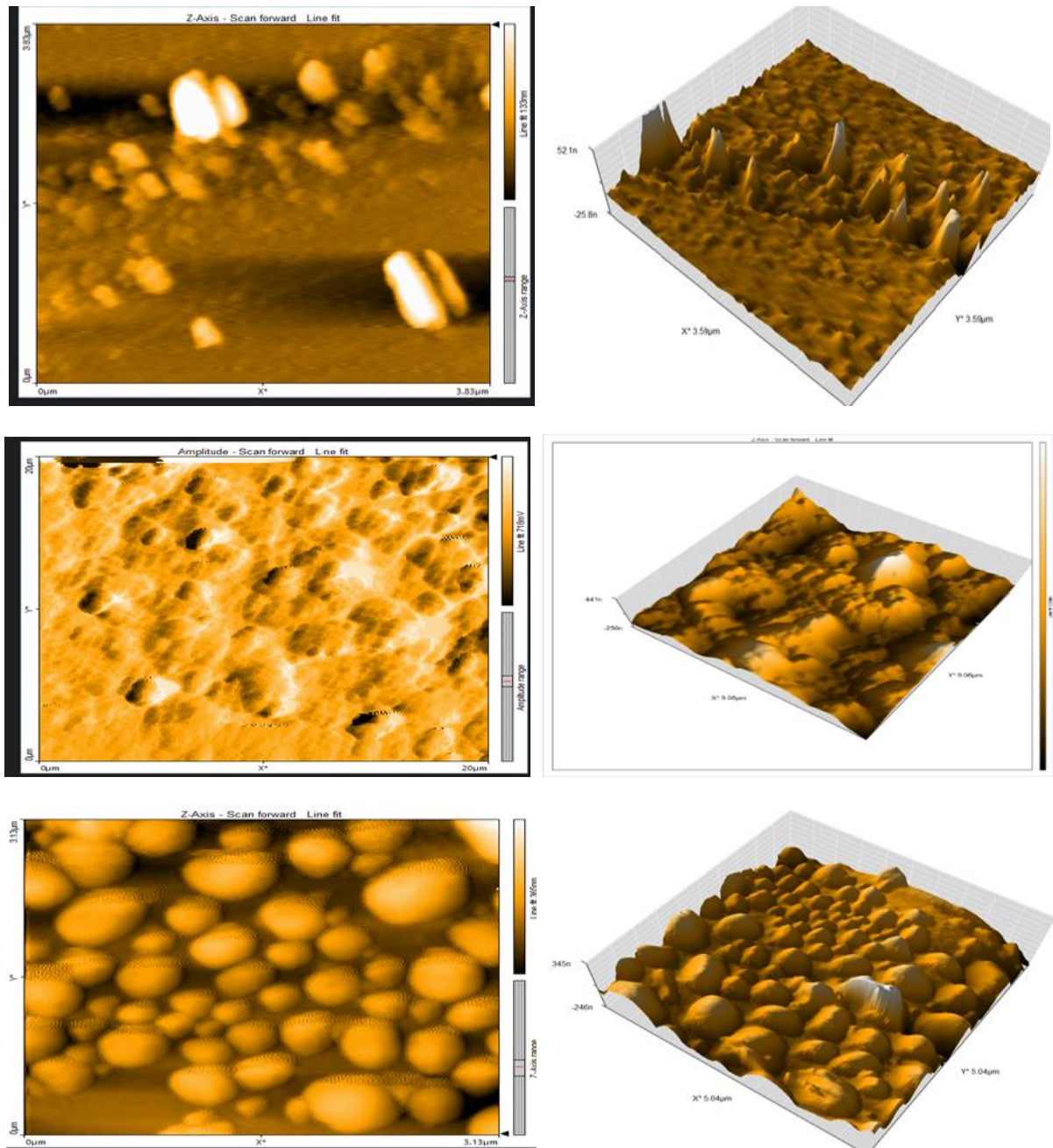


Figure 7: AFM images for (a) PE, (b) PE with n-ZnO, and (c) PE with n-TiO₂

Table 5: AFM parameters to coated SS304L with PE in without and in the presence of the nanomaterials

| System | Ra (nm) | RMS (nm) | Mean grain size (nm) |
|---------------------------------------|---------|----------|----------------------|
| Coated by polymer PE | 8.360 | 9.302 | 103.7 |
| coated of polymer PE+ZnO | 4.879 | 5.897 | 98.56 |
| Coated of polymer PE+TiO ₂ | 4.523 | 5.236 | 96.58 |

Table 6: PE polymer inhibition zone with and without nanomaterial

| Coating | Gram-positive <i>S. aureus</i> | Gram-negative <i>E. coli</i> |
|---------------------|-----------------------------------|---------------------------------|
| PE | 14 | 18 |
| PE+ZNO | 30 | 30 |
| PE+TiO ₂ | 28 | 24 |
| Amoxicillin | 30 | 30 |
| DMSO | - | - |

The polymer showed the superior inhibitory effectiveness against both *S. aureus* and *E. coli* when compared to amoxicillin. The polymer's capacity to kill bacteria is determined by the stable interaction complex produced between the cleaved DNA and the drug-bound topoisomerases. The cell's ability to tolerate DNA-damaging medicines [27] demonstrates how the polymer's inhibition of topoisomerase activity and the creation of stable complexes with DNA have a substantial negative effect on the cell. Nanomaterials are becoming more important in pharmaceutical and biological applications as an antibacterial strategy against the proliferation of infectious diseases and the increase of antibiotic-resistant strains [28]. Due to the combination of their high surface to volume ratio and small size, which enables them to close contacts with microbial membranes, nanomaterials are regarded as the efficient biocides.

Conclusion

In 3.5% of NaCl solution, the electro polymerization of PE on SS 304L served as an effective anti-corrosion coating. The efficiency of protection (Pe%) and corrosion polarization resistance (Rp) of the coating polymer decrease by increasing temperature and the Pe% increases after adding nanomaterials, particularly ZnO. The corrosion potential was working as anodic protection and was moving in the noble direction. According to the FAM study, the protection of the SS 304L under investigation is caused by the development of a protective coating on the SS

304L surface. In addition, the biological activity of polymer film (PE) modified with nanomaterial has moderate activity against Gram-negative bacteria (*E. coli*) and Gram-positive bacteria (*B. subtilis*) (*S. aureus*).

Funding

This research did not receive any specific grant from funding agencies in the public, commercial, or not-for-profit sectors.

Authors' contributions

All authors contributed to data analysis, drafting, and revising of the paper and agreed to be responsible for all the aspects of this work.

Conflict of Interest

The author declared that they have no conflict of interest.

References

[1]. Darafarin M., Eslami H., Raoufian E., Electropolymerization of styrene in alcoholic solution and preparation of its bilayer with polyacrylamide, *Polymer Bulletin*, 2019, **76**:3003 [[Crossref](#)], [[Google Scholar](#)], [[Publisher](#)]
[2]. Rojo L., Vazquez B., Parra J., López Bravo A., Deb S., San Roman J., From natural products to polymeric derivatives of “eugenol”: A new approach for preparation of dental composites and orthopedic bone cements, *Biomacromolecules*, 2006, **7**:2751 [[Crossref](#)], [[Google Scholar](#)], [[Publisher](#)]

- [3]. Darafarin M., Eslami H., Raoufian E., Electropolymerization of styrene in alcoholic solution and preparation of its bilayer with polyacrylamide, *Polymer Bulletin*, 2019, **76**:3003 [[Crossref](#)], [[Google Scholar](#)], [[Publisher](#)]
- [4]. Yağan A., Corrosion performances of polyaniline and poly (N-methylaniline) coated stainless steel by impedance spectroscopy, *Int. J. Electrochem. Sci.*, 2019, **14**:2906 [[Crossref](#)], [[Google Scholar](#)], [[Publisher](#)]
- [5]. Chamovska D., Porjazoska-Kujundziski A., Grchev T., Polypyrrole coatings for corrosion protection of stainless steel, *Zaštita materijala*, 2013, **54**:229 [[Google Scholar](#)], [[Publisher](#)]
- [6]. Llevot A., Grau E., Carlotti S., Grelier S., Cramail H., From lignin-derived aromatic compounds to novel biobased polymers, *Macromolecular rapid communications*, 2016, **37**:9 [[Crossref](#)], [[Google Scholar](#)], [[Publisher](#)]
- [7]. Khalil A.A., ur Rahman U., Khan M.R., Sahar A., Mehmood T., Khan M., Essential Oil Eugenol: Sources, Extraction Techniques and Nutraceutical Perspectives, *RSC advances*, 2017, **7**:32669 [[Crossref](#)], [[Google Scholar](#)], [[Publisher](#)]
- [8]. Kouznetsov V.V., Vargas Méndez L.Y., Synthesis of eugenol-based monomers for sustainable epoxy thermoplastic polymers, *Journal of Applied Polymer Science*, 2022, **139**:52237 [[Crossref](#)], [[Google Scholar](#)], [[Publisher](#)]
- [9]. Ali M.I., Saleh K.A., Electropolymerization of N-Salicyly tetrahydro phthalamic acid for anticorrosion and antibacterial action applications, In *IOP Conference Series: Materials Science and Engineering*, 2019, **571**:012072 [[Crossref](#)], [[Google Scholar](#)], [[Publisher](#)]
- [10]. Kenawy E.R., Worley S.D., Broughton R., The Chemistry and applications of antimicrobial polymers: A State-of-the-Art Review, polymers of high molecular weight have been used, *Biomacromolecules*, 2007, **8**:1359 [[Crossref](#)], [[Google Scholar](#)], [[Publisher](#)]
- [11]. Al-Mashhadani H.A., Saleh K.A., Electro-polymerization of poly Eugenol on Ti and Ti alloy dental implant treatment by micro arc oxidation using as Anti-corrosion and Anti-microbial, *Research Journal of Pharmacy and Technology*, 2020, **13**:4687 [[Crossref](#)], [[Google Scholar](#)], [[Publisher](#)]
- [12]. Gleiter H., Nanostructured materials: basic concepts and microstructure, *Acta materialia*, 2000, **48**:1 [[Crossref](#)], [[Google Scholar](#)], [[Publisher](#)]
- [13]. Fathi, A.M., Mandour H.S., Electrosynthesized conducting poly (1, 5-diaminonaphthalene) as a corrosion inhibitor for copper, *Polymer Bulletin*, 2020, **77**:3305 [[Crossref](#)], [[Google Scholar](#)], [[Publisher](#)]
- [14]. Saleh K.A., Ali M.I., Electro polymerization for (N-Terminal tetrahydrophthalamic acid) for Anti-corrosion and Biological Activity Applications, *Iraqi Journal of Science*, 2020, **61**:1 [[Crossref](#)], [[Google Scholar](#)], [[Publisher](#)]
- [15]. Saleh J.M., Al-Haidari Y.K., Inhibiting effects of ethanethiol, dimethyl sulfide, and dimethyl disulfide on the corrosion of stainless steel (405) in sulfuric acid, *Bulletin of the Chemical Society of Japan*, 1989, **62**:1237 [[Crossref](#)], [[Google Scholar](#)], [[Publisher](#)]
- [16]. Al-Rudaini K.A.K., Al-Saadie, K.A.S., Study the Corrosion behavior of AA7051 Aluminum alloy at different temperatures and inhibitor concentration in Acidic medium, *Research Journal of Pharmacy and Technology*, **14**:4977 [[Crossref](#)], [[Google Scholar](#)]
- [17]. Joseph B., John S., Joseph A., Narayana B., Imidazolidine-2-thione as corrosion inhibitor for mild steel in hydrochloric acid, *Indian Journal of Chemical Technology (IJCT)*, 2010, **17**:366 [[Crossref](#)], [[Google Scholar](#)], [[Publisher](#)]
- [18]. Habeeb S.A., Saleh K.A., Electrochemical Polymerization and Biological Activity of 4-(Nicotinamido)-4-Oxo-2-Butenoic Acid as An Anticorrosion Coating on A 316L Stainless Steel Surface, *Iraqi Journal of Science*, 2021, **62**:729 [[Crossref](#)], [[Google Scholar](#)], [[Publisher](#)]
- [19]. Mohammed R.A., Saleh K.A., Advanced anticorrosive coating prepared from poly [N-(Pyridine-2-yl) maleamic acid]/graphene derivatives nanocomposites, *Materials Today: Proceedings*, 2022, **61**:805 [[Crossref](#)], [[Google Scholar](#)], [[Publisher](#)]
- [20]. Kumar S.A., Sankar A., Kumar S.R., Vitamin B-12 Solution as Corrosion Inhibitor for Mild Steel in Acid Medium, *International Journal of*

- Electrochemical Science*, 2013, **3**:57 [[Crossref](#)], [[Google Scholar](#)], [[Publisher](#)]
- [21]. Al-sammarraie A.M., Shaker R.A., Corrosion protection enhancement of; zn, cu, al, carbon steel and stainless steel 316 artificial seawater by coating with nanomaterials, 2014, M.Sc. Thesis. College of science, University of Baghdad [[Crossref](#)], [[Google Scholar](#)], [[Publisher](#)]
- [22]. Oliveira M.A.S., Moraes J.J., Faez R., Impedance studies of poly (methylemethacrylate-co-acrylic acid) doped polyaniline films on aluminum alloy, *Progress in Organic Coatings*, 2009, **65**:348 [[Crossref](#)], [[Google Scholar](#)], [[Publisher](#)]
- [23]. Mohammed R., Saleh K., A novel conducting polyamic acid/nanocomposite coating for corrosion protection, *Eurasian Chemical Communications*, 2021, **3**:715 [[Crossref](#)], [[Google Scholar](#)], [[Publisher](#)]
- [24]. Abdallah M., Rhodanine azosulpha drugs as corrosion inhibitors for corrosion of 304 stainless steel in hydrochloric acid solution, *Corrosion science*, 2002, **44**:717 [[Crossref](#)], [[Google Scholar](#)], [[Publisher](#)]
- [25]. Noor E.A., Al-Moubaraki A.H., Thermodynamic study of metal corrosion and inhibitor adsorption processes in mild steel/1-methyl-4 [4'(-X)-styryl pyridinium iodides/hydrochloric acid systems, *Materials Chemistry and Physics*, 2008, **110**:145 [[Crossref](#)], [[Google Scholar](#)], [[Publisher](#)]
- [26]. Alves K.G.B., Felix J.F., de Melo E.F., dos Santos C.G., Andrade C.A., de Melo C.P., Characterization of ZnO/Polyaniline nanocomposites prepared by using surfactant solutions as polymerization media, *Journal of Applied Polymer Science*, 2012, **125**:E141 [[Crossref](#)], [[Google Scholar](#)], [[Publisher](#)]
- [27]. Kohanski M.A., Dwyer D.J., Collins J.J., How Antibiotics Kill Bacteria: from Targets to Networks, *Nature Reviews: Microbiology*, 2010, **8**:423 [[Crossref](#)], [[Google Scholar](#)], [[Publisher](#)]
- [28]. Abd El-Rehim S.S., Hassan H.H., Amin M.A., Corrosion inhibition of aluminium by 1, 1(lauryl amido) propyl ammonium chloride in HCl solution, *Materials chemistry and physics*, 2001, **70**:64 [[Crossref](#)], [[Google Scholar](#)], [[Publisher](#)]

HOW TO CITE THIS ARTICLE

Ayat Monther Alqudsi, Khulood Abed Saleh, Electrochemical Polymerization of Eugenol and Corrosion Protection Studies of Stainless Steel 304L Alloy. *J. Med. Chem. Sci.*, 2023, 6(8) 1818-1829

DOI: <https://doi.org/10.26655/JMCHMSCI.2023.8.10>

URL: http://www.jmchemsci.com/article_164180.html